STUDENT SESSION

S1

THERMAL STABILITY OF TITANATE NANOTUBES

D. Králová[1], R. Kužel[2], J. Kovářová[1], J. Dybal[1], M. Šlouf[1]

[1]*Institute of Macromolecular Chemistry, Academy of Sciences of the Czech Republic, Heyrovskeho nam. 2, 162 06 Praha 6, Czech Republic*
[2]*Department of Condensed Matter Physics, Faculty of Mathematics and Physics, Charles University, 121 16 Praha 2, Ke Karlovu 5, Czech Republic*
kralova@imc.cas.cz

Titanate nanotubes (Ti-NT) were prepared by hydrothermal synthesis from four different TiO_2 powders: anatase micropowder (mA), rutile micropowder (mR), anatase nanopowder (nA), and rutile nanopowder (nR). As we use the nanotubes as filler in molten polymers, we investigated their structural changes at elevated temperatures (up to 800 °C) by a number of methods: transmission electron microscopy (TEM), selected-area electron diffraction (SAED), powder X-ray diffraction (PXRD), thermogravimetric analysis (TGA) and Raman scattering (RS). The shapes of nanotubes were not changed as proved by TEM. The structure of single sheets, from which the nanotubes were formed, was also stable as confirmed by SAED at high scattering vectors q. Packing of sheets and chemical bonding between the sheets was, however, strongly dependent on the temperature, as indicated by PXRD at low q, TGA and RS.

Introduction

In the past decade, titanate nanotubes (Ti-NT) have attracted much attention because of their interesting structure, morphology and potential applications. A few studies have reported also their thermal stability at high temperatures. Basically, all were in agreement that structure of Ti-NT was stable until about 300 °C. Above this temperature, the crystalline structure of Ti-NT changed, usually

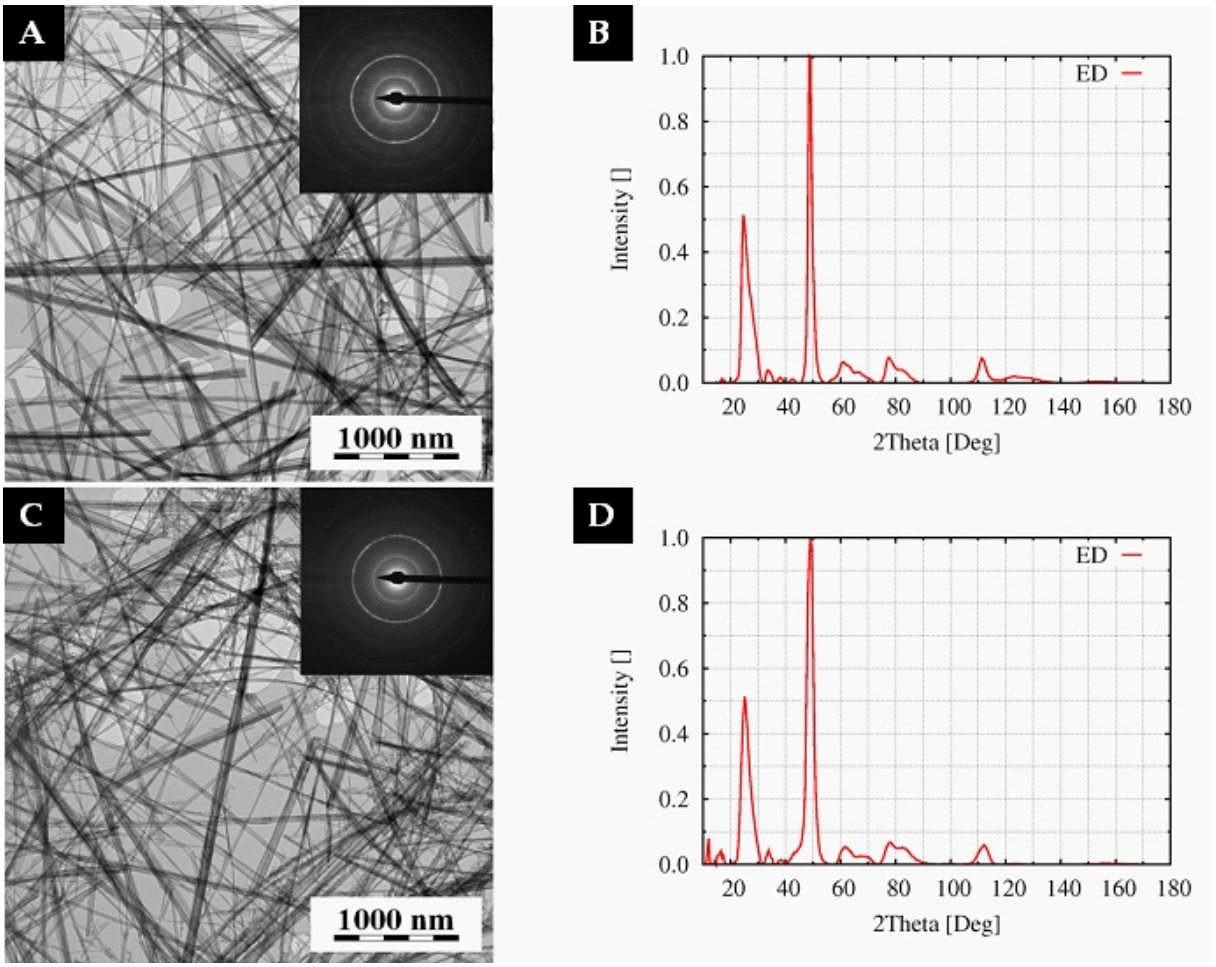

Figure 1. TEM micrographs and ED patterns of Ti-NT heated up to 300°C (a,b) and non-heated Ti-NT (c,d); no significant difference was observed.

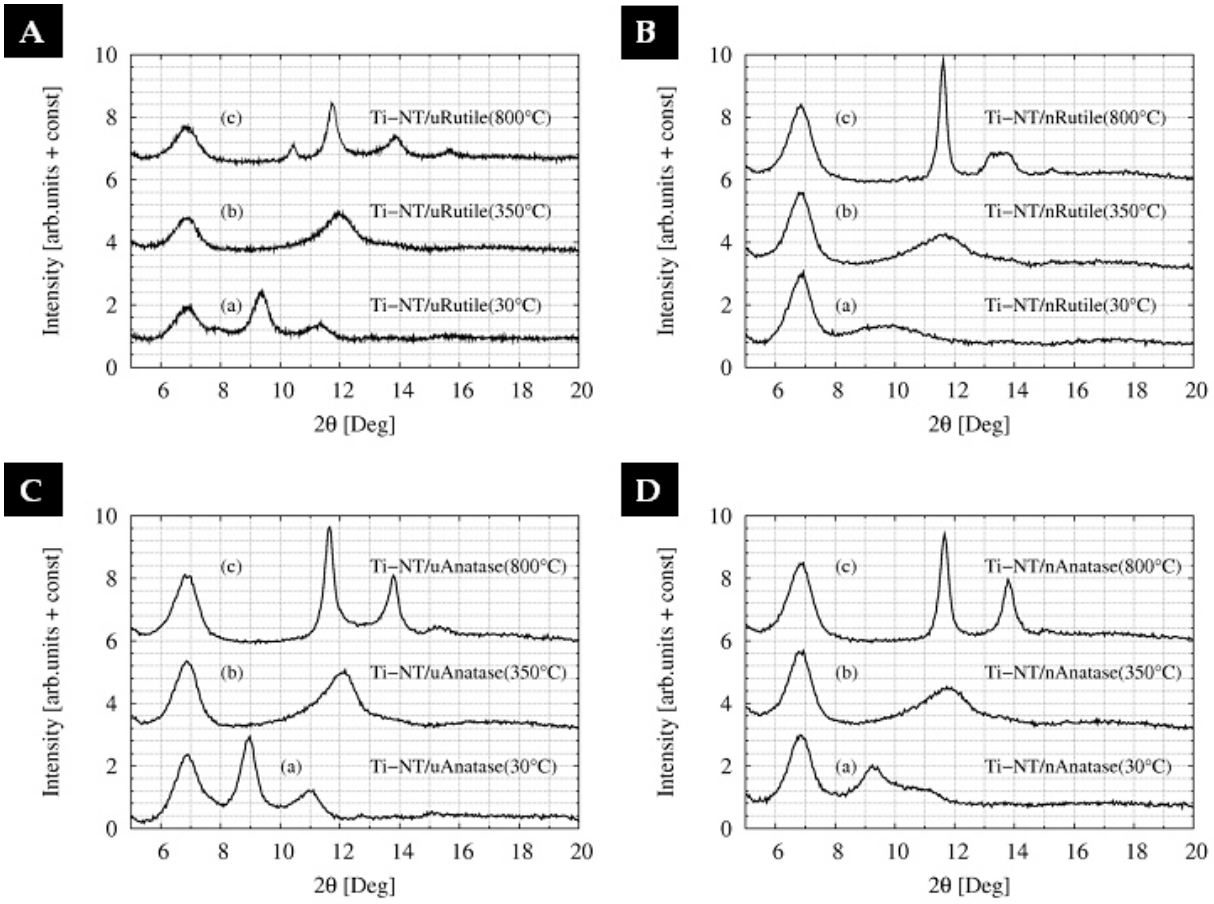

Figure 2. PXRD of Ti-NT synthesized from micro-rutile (A), nano-rutile (B), micro-anatase (C) and nano-anatase showed significant changes.

into anatase or rutile [1-5]. The aim of this work was to confirm morphological stability of Ti-NT at elevated temperatures that we used during polymer composites preparation. Moreover, we wanted to compare the differences among Ti-NT synthesized from various TiO_2 crystal sizes and modifications.

Experimental

Titanate nanotubes (Ti-NT) were synthesized by hydrothermal synthesis as reported in our previous work [6]. Briefly, Ti-NT were synthesized from four different TiO_2 powders (anatase micropowder (mA), rutile micropowder (mR), rutile nanopowder (nR), and anatase nanopowder (nA)). Initial concentration of TiO_2 was 0.1 g; reaction time was 48 hours.

The morphology of the nanotubes was investigated by TEM. A droplet of the Ti-NT aqueous suspension was deposited on a carbon-coated copper grid, left to evaporate and then inspected in a transmission electron microscope (TEM; Tecnai G^2 Spirit 120, FEI, Czech Republic). For investigation of thermal stability, specimens prepared on TEM grids were heated at 300 °C for 1 hour and then observed in TEM. The crystalline structure at high scattering angles $q > 1.4$ Å^{-1} was obtained from SAED on the same microscope.

The crystalline structure and its thermal stability was also characterized by powder X-ray diffraction (PXRD, diffractograms at low scattering angles $q < 1.4$ Å^{-1}, temperatures up to 800 °C with step of 50 °C, each temperature was hold for 1 h before measurement), thermogravimetric analysis (TGA, analyses up to 800 °C, heating rate 5 °C/min) and Raman microscopy (RS, temperature up to 350 °C, step 50 °C heating rate 10 °C/min, temperature held 10 min before each measurement).

Results

TEM micrographs (Fig. 1a, c) proved that Ti-NT morphology was not affected by heating up to 300 °C, which was the maximum temperature used during melt mixing of polymer composites with Ti-NT. It has been demonstrated [7] that Ti-NT are formed by rolled sheets, which are composed of titania octahedra. The periodic distances within the sheets are low and so the corresponding diffractions are observed at high scattering vectors (q > 1.4 Å^{-1} 2 (CuK) > 20°), whereas interplanar distances within the rolled sheet are in the range of nanometers, which corresponds to lower scattering vectors (q < 1.4 Å^{-1} 2 (CuK) < 20°). The periodic interatomic distances within single sheets, observed at high q by SAED, did not change (Fig. 1b, d). On the other hand, the interplanar distances due to rolling of the sheets, observed at low q by PXRD, exhibited significant shifts (Fig. 2). Moreover, changes at elevated temperatures, indicated by PXRD, were confirmed by TGA (decrease of sample mass with the temperature, most likely release of water) and also by RS (change of Raman spectra starting at 150 °C).

Conclusion

The morphology of our laboratory-synthesized titanate nanotubes was stable at elevated temperatures (up to 300 °C) as proved by TEM (Fig.1a, c). The crystal structure of single sheets was also stable, as confirmed by SAED (Fig.1b, d). Packing of sheets and chemical bonding between the sheets was, however, strongly dependent on the temperature, as indicated by PXRD at low *q* (Fig. 2). Structural changes at elevated temperatures were proved also by TGA and RS.

References

1. E. Morgado Jr., M. A.S. de Abreu, O. R.C. Pravia, B. A. Marinkovic, P. M. Jardim, F. C. Rizzo, A. S. Araújo, *Solid State Sciences,* **8**, (2006), 888.
2. L.-Q. Weng, S.-H. Song, S. Hodgson, A. Baker, J. Yu, *Journal of the European Ceramic Society,* **26**, (2006), 1405.
3. Y. Lan, X. Gao, H. Zhu, Z. Zheng, T. Yan, F. Wu, S. P. Ringer, D. Song, *Adv. Funct. Mater*., **15**, (2005), 1310.
4. W. Wang, O. K. Varghese, M. Paulose, and C. A. Grimes, Q. Wang and E. C. Dickey, *J. Mater. Res*., **19**, no. 2, (2004)
5. Y.-F. Chena, C.-Y. Lee, M.-Y. Yeng, H.-T. Chiu*, Materials Chemistry and Physics,* **81**, (2003), 39.
6. D. Králová, M. Šlouf, R. Kužel, *Materials Structure*, **15**, no. 2a, (2008), k60.
7. B. D. Yao, Y. F. Chan, X. Y. Zhang, W. F. Zhang, Z. Y. Yang, and N. Wang, *Appl. Phys. Lett*., **82**, No. 2, (2003), 281.

Acknowledgements

Financial support through grants KAN200520704 a GACR 203/07/0717 is gratefully acknowledged.

S2

XRD STUDY OF THICKNESS DEPENDENCE OF CRYSTALLIZATION AND STRESSES OF TiO_2 THIN FILMS

L. Nichtová[1], R. Kužel[1], Z. Matěj[1], J. Šícha[2]

[1]Department of Condensed Matter Physics, Facuty of Mathematics and Physics, Charles University in Prague, 121 16 Praha 2, Czech Republic, nichtova@email.cz
[2]Department of Physics, Facuty of Applied Sciences, University of West Bohemia in Pilsen

Titanium dioxide is a material intensively investigated not only because of its good chemical stability, mechanical hardness, high refractive index and nontoxicity but also due to its photocatalytic activity enabling a conversion of solar light into useful chemical energy. It is known that photocatalytic activity of titanium dioxide strongly depends on crystallization and phase composition.

In this work a complex X-ray diffraction (XRD) study of thin TiO_2 films on Si substrates with different thicknesses (50 2000 nm) prepared by magnetron sputtering is presented. Crystallisation process of amorphous films was studied in-situ. XRD reflectivity, texture and stress measurements were performed ex-situ. Other amorphous and nanocrystalline powders were also measured for comparison.

In-situ xrd measurements were done with the aid of X'Pert Pro diffractometer with MRI high-temperature chamber. Annealing temperatures were selected below the temperature where fast crystallization appears (about 220 °C). The process is then slow and allows detailed time in-situ investigations even in laboratory conditions. Strong dependence of crystallization kinetics on the film thickness was found. In particular for the samples with thickness lower than 300 nm. The process could be well described by the Avrami equation [1] (modified by the introduction of initial time of crystallization). The evolution of the integrated intensities *I* (Figure 1) of diffraction lines of anatase phase is then described as, $I = 1\text{-}exp[-b(t-t_0)^n)]$, where the initial time of crystallization t_0 is related to the first appearance of any diffracted intensity above the background level at the peak position. It increases abruptly with decreasing thickness. The rate of crystallization *b* grows quickly with the thickness. Low values of *n* (~ 2) indicate two-dimensional character of the crystallite growth. Changes of preferred orientation and stress generation during the crystallization were observed.

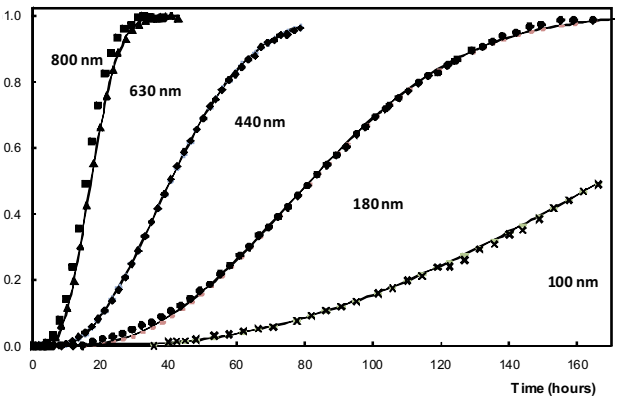

Figure 1. Normalized integrated intensity of anatase diffraction peak 101 in dependence on annealing time (annealing temperature 180 °C) for films of different thickness (symbols … experimental values, lines … fitted Avrami equations).

Tensile residual stresses were developed slowly during the crystallization and confirmed later by detailed measure-

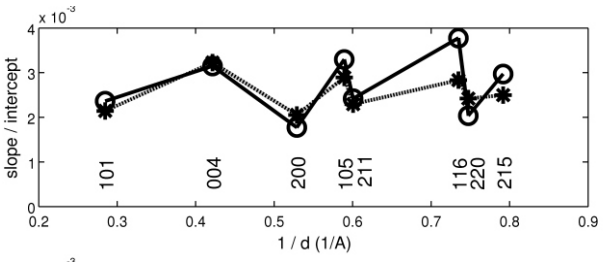

Figure 2. Comparison of slopes divided by corresponding intercepts of the sin^2 plots for the 440 nm thin film sample (o) and simulated XECs anisotropy dependence (*).

ments at room temperature. In the first step, the stress measurements were analysed with X'Pert Stress program by means of the d_{hkl} vs. sin^2 plots. Slopes and intercepts of the sin^2 plots were obtained. In the second step, the stress values were determined from the analysis of all the reflections assuming symmetrical bi-axial state of the residual stress and the weighted Reuss- Voigt grain interaction model [2]. Figure 2 shows obtained and calculated slopes divided by the corresponding intercepts of the sin^2 plots for all measured reflections for the sample with thickness

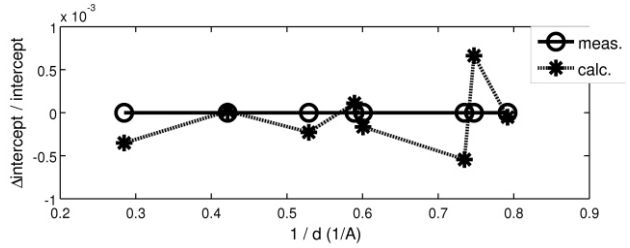

Figure 3. Relative differences of intercepts of sin^2 plots for the 440 nm thin film sample (o) and simulated data (*).

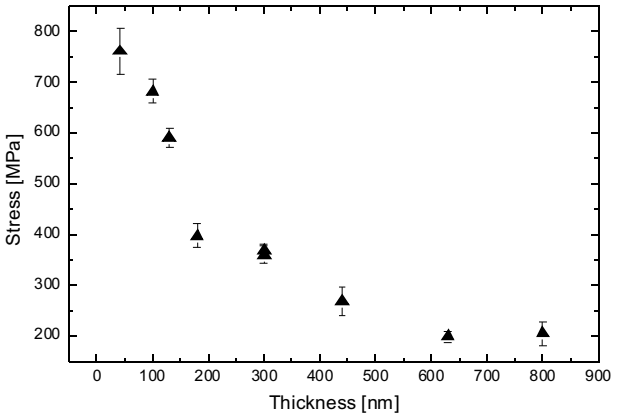

Figure 4. Film thickness dependence of the residual stress.

440 nm annealed at 200 C. Systematic anisotropy, observed for all investigated samples, can be well described by the weighted Reuss-Voigt model using single crystal elastic constants of anatase [3] which recently appeared. The anisotropy is completely different for rutile – the second phase of tetragonal TiO_2. Figure 3 shows relative deviation of obtained and calculated sin^2 intercepts. Deviations are rather small, comparable with the rounding error of the intercepts values in the X'Pert Stress program. Rapidly increasing value of residual stress with decreasing film thickness was observed (Figure 4).

1. M. J. Avrami, *J. Chem. Phys.* **7** 1103 (1939).
2. M. Dopita, D. Rafaja, *Z. Kristallogr.* Suppl. **23** (2006) 67-72.
3. M. Iuga, G. Steinle-Neumann, J. Meinhardt, *Eur. Phys. J.* **B58** (2007) 127-133.

S3

PAIR DISTRIBUTION FUNCTION OF NANOPOWDERS

J. Dolinár, S. Daniš

Department of Condensed Matter Physics, Faculty of Mathematics and Physics, Charles University in Prague, Czech Republic, jan.dolinar@matfyz.cz

PDF is method developed almost 80 years ago, but until recently it was applied almost exclusively on amorphous materials and liquids. Nowadays, when high quality data from synchrotrons a neutron sources are available, it is becoming a popular method also for research of crystalline materials. Usually only high energy radiation sources are used, because wide Q-space interval measurement is needed in order to produce good resolution in the real space PDF. Despite this, some authors (see [1,2]) admit that it may be possible in some applications to obtain useful data using regular laboratory X-ray sources. In case of nanoparticles this would be especially helpful as it would allow very convenient way of studying some of their properties that are not accessible from reciprocal space experiments.

Our aim is to prove this possibility and to develop necessary tools and methods. Our equipment consists of HZG4 theta-2theta goniometer, molybdenum X-ray tube as a radiation source and simple scintillation detector. The process of converting measured intensities $I(q)$ into real space pair distribution function $g(r)$ is in our case rather simple and straightforward. The combination of low energy beam and nanopowder sample, allows to neglect many of the corrections that usually have to be carried out in ordinary PDF experiments. At the present moment our calculations account only for background correction, K_2 separation and various scaling and normalization adjustments. Polarization correction is planned in very near future. In spite of this simplicity, very satisfactorily results were obtained.

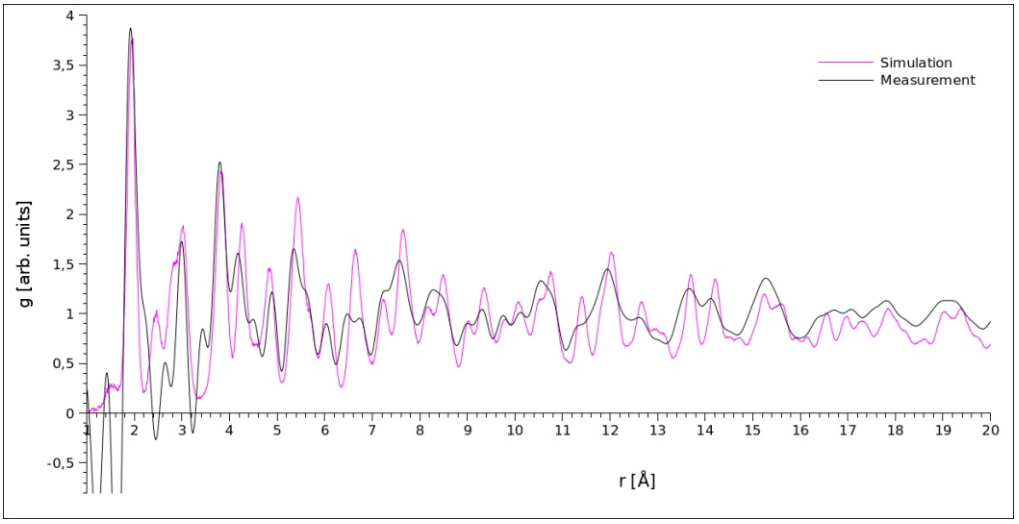

Figure 1. Comparison of PDF calculated from measurement of TiO_2 nanoparticles with simulated PDF. Note the incorrect shape of peaks in simulated line caused by inaccurate model.

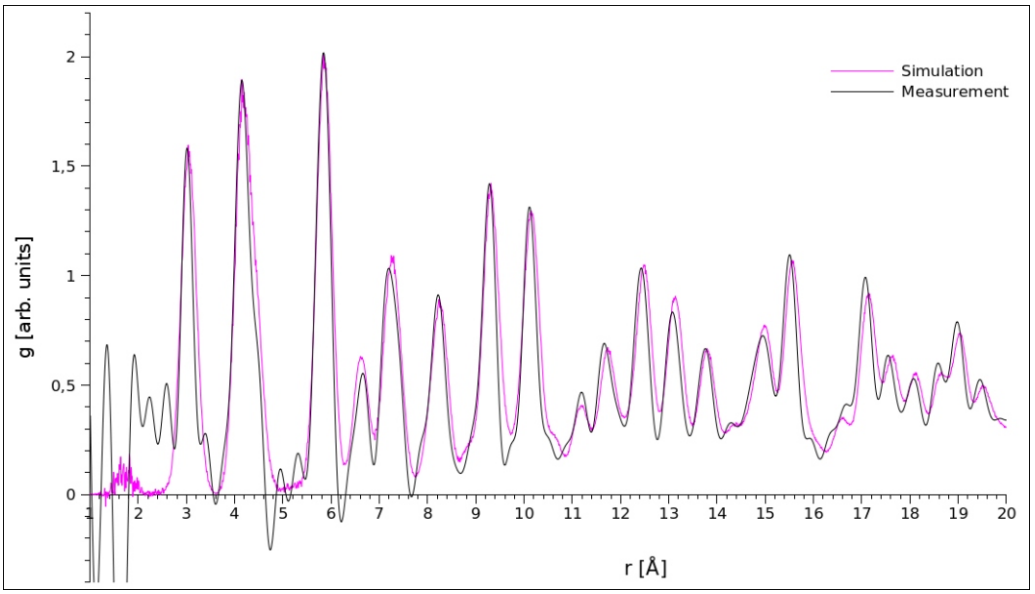

Figure 2. Comparison of PDF calculated from measurement of crystalline LaB_6 with simulated PDF.

To confirm the quality of calculated PDF various simulations were made and compared to data obtained from measurement. One of such comparisons carried out for TiO_2 nanoparticles in anatase phase is presented in Fig. 1. Note that although most of the features in simulated PDF are at same positions as in measured data, only the shape of the peaks is different. This disagreement is not due to errors in PDF calculation, but rather a flaw of nanoparticle model used in simulation. To support this statement we attach the very same comparison performed on LaB_6 crystalline powder in Fig 2. In this case, model of bulk material was used in simulation, as is appropriate for m-sized crystallites.

Further goals are to develop better apparatus for theoretical simulations, fine-tune the calculation of PDF and also adapt our hardware to allow faster, easier and more precise data collection. After the method is ready and reliable, we plan to study nanoparticle specific defects, like surface deformations.

1. T. Egami, S.J.L. Billinge, *Underneath the Bragg peaks: structural analysis of complex materials.* New York: Elsevier. 2003.

2. Th. Proffen, S. J. L. Billinge, T. Egami and D. Louca, *Z. Kristallogr.*, **218**, (2003), 132-143.

S4

STUDY OF THE PHASE COMPOSITION OF Fe_2O_3 NANOPARTICLES

Václav Valeš[1], Jana Poltierová-Vejpravová[1], Petr Brázda[2], Alice Mantlíková[1], and Václav Holý[1]

[1]Department of Condensed Matter Physics, Faculty of Mathematics and Physics, Charles University in Prague, Czech Republic
[2]Department of Inorganic Chemistry, Faculty of Science, Charles University in Prague, Czech Republic

Introduction

Important physical properties of nanoparticles are determined mainly by their atomic structure, especially by their phase composition and the presence of structure defects. X-ray diffraction is a good tool for studying the structure of the nanoparticles, its application for very small particles is however limited by very small intensity of the scattered wave. For this reason special experimental setups, like e.g. diffraction with small incidence angle, are used and many experiments have to be done at synchrotrons. Standard methods of the measured data analysis based on the description of the diffraction using instrumental functions and functions of physical broadening of the lines fail in the case of very small particles. An ab-initio calculation method (based on the Debye formula [1, 2]) has to be used instead.

In this work the Debye formula is used for the description of the diffraction of iron oxide samples measured at ANKA synchrotron in Karlsruhe. Using this approach we determine basic parameters of the particles such as lattice parameters and the size of the particles, as well as the presence of different phases. During annealing, subsequent phase transitions from -Fe_2O_{34} to -Fe_2O_3 and to -Fe_2O_3 take place. New phases nucleate probably at the surface of the nanoparticles and the phase transformation proceeds towards the particle center ([3, 4]), so that the structure of the nanoparticles can be described by a core-shell model; this model was used in the Debye-formula based simulation. From the analysis of the experimental data we determined the kinetic parameters of the phase transitions and their dependence on the nanoparticle sizes.

Measured samples

The great interest in Fe_2O_3 nanoparticles is caused mainly by magnetic properties of these particles, namely extremely high room temperature coercivity of epsilon phase of these iron oxide nanoparticles. The samples were prepared by ex-situ annealing of organic precursors and then measured at ANKA synchrotron in Karlsruhe with incidence angle 5 and the wavelength of 0.95007 Å. The primary beam was monochromatized by a 2 111 Si monochromator, the diffracted radiation was measured by a point detector equipped with a narrow entrance slit and a filter suppressing the Fe-fluorescence. The series of samples was prepared with the final annealing temperature from 900 C to 1150 C with the step of 50 C. To the temperature of 900 C all the samples were heated at the speed 1 C per minute and stayed at this temperature for 4 hours. As for the sample with the final temperature 900 C this was the whole procedure. The other samples were then with the same speed heated to their final annealing temperature with the 4-hour waiting each 50 C up to their final heating temperature. This procedure causes the creation of Fe_2O_3 nanoparticles in the amorphous SiO_2 matrix. From the literature [5] it is known that the particles created at the lowest final temperature should be in the form of maghemite and with increasing final temperature the phase of Fe_2O_3 particles should change to and hematite.

Theoretical description

Debye formula in Eq. (1), which has been used for the X-ray data analysis describes the intensity distribution of the samples consisting of the same randomly oriented particles, knowing the positions of the atoms in one such a particle.

$$I(Q) \quad \sum_{i,j} f_i f_j^* \frac{\sin(Qr_{ij})}{Qr_{ij}}, \qquad (1)$$

where the double sum goes over all atoms in the particle, Q is the length of the scattering vector, f_i is the atom form factor of the i-th atom and r_{ij} is the distance between i-th and j-th atom. The formula is valid for any arrangement of atoms in any particle; no lattice is needed; only exact positions of atoms in the particle are important. The only technical limit of using of this equation is the number of terms in the double sum. For instance, a particle of Fe_2O_3 of diameter of 13 nm contains about 10^5 atoms, which means that there are 10^{10} interatomic distances that have to be

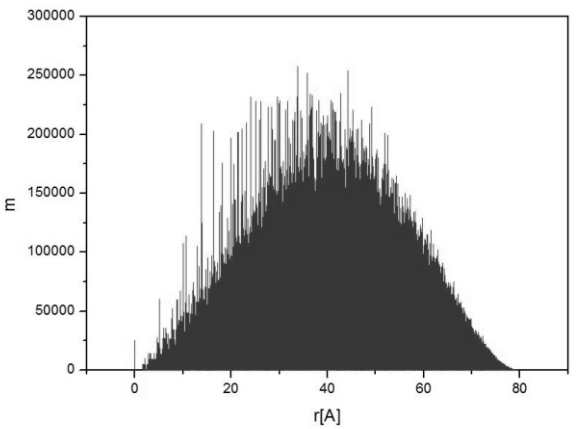

Figure 1. Calculated histogram of interatomic distances in a spherical Fe_2O_3 particle of radius of 40 Å. The histogram step is 0.01 Å.

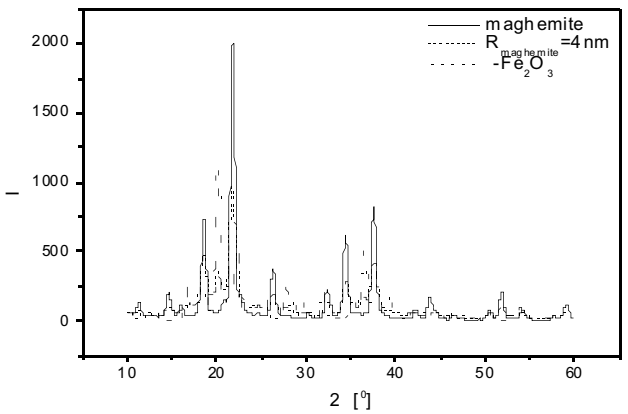

Figure 2. Calculation of diffraction curves for different phases of Fe_2O_3. The full line corresponds to the pure maghemite particle of radius of 50 Å; the dotted one to the pure -Fe_2O_3 particle of the same radius; and the dashed line represents the diffraction from the particles of radius 50 Å, which consist of the core (radius 40 Å) of maghemite and the shell of -Fe_2O_3.

taken into account for every Q. For this reason, the distribution function of atomic pairs was calculated and a histogram of all interatomic distances was created; an example of such histogram is shown in Fig. 1 corresponding to a spherical particle with the radius of 40 Å, the histogram has been constructed using the step width of 0.01 Å.

Since we introduced the histogram of interatomic distances, we can rewrite the Eq. (1) using calculated data from the histogram, i.e. we know the multiplicity of each of interval of distances. The rewritten form of Debye formula in equation (2) enables us to perform calculations for much larger samples. For the intensity we can write

$$I(Q) \quad \sum_{i,j} m_i |f|^2 \frac{\sin(Qr_{ij})}{Qr_{ij}}, \qquad (2)$$

where m_i is the multiplicity factor for the i-th interval of distances. The expression in Eq. (2) is valid only for one type of atoms in the particle, which is not our case (because of different atom form factors). This fact requires only some technical changes, which do not affect the fundamental meaning of Eq. (2).

The phase transition from one phase to the other is supposed to take place from the particle surface to its center. For this reason the core-shell model of the particle (particle consisting of two different phases) has been introduced to the Debye formula program. In order to have a brief look in to the behavior of the simulated data calculated by our model, diffraction curves for different phases were calculated (Fig. 2). From this picture the difference between the maghemite and phases of Fe_2O_3 can be seen as well as the effect of the core-shell structure of these two phases, which causes some "mixture" of the diffraction pattern of both phases.

Data analysis

Several samples from the series described above were analysed by the Debye-formula approach using the core-shell model, assuming that the interface of the two phases moves from the surface to the center of the particle. The data from the Figs. 3 5 (samples A–C) were fitted by hand and the results are summarized in Table 1; the errors were estimated from this fit too. The background was approximated ad-hoc by a polynomial of the third power. The broad peak around 13 is caused by the amorphous SiO_2 matrix and for

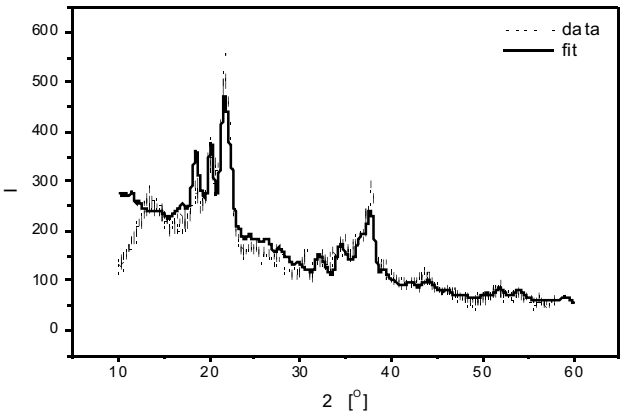

Figure 3. Sample A. Measured data and fit of the sample annealed at the 900 C as the highest temperature.

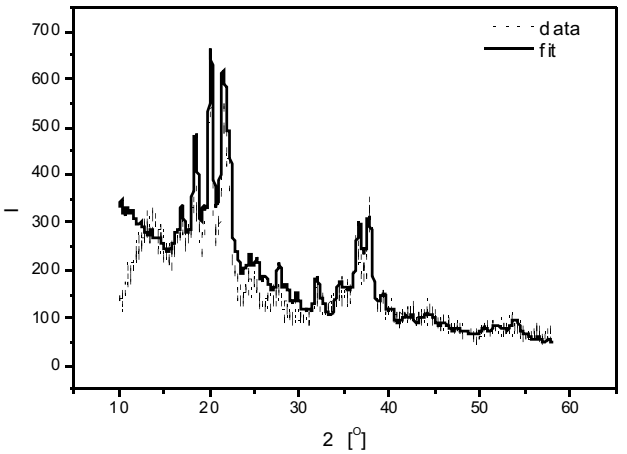

Figure 4. Sample B. Measured data and fit of the sample annealed at the 950 C as the highest temperature.

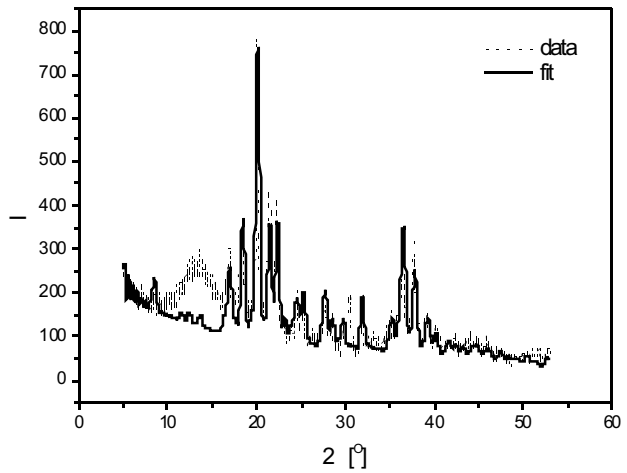

Figure 5. Sample C. Measured data and fit of the sample annealed at the 1000 C as the highest temperature.

Table 1. Results obtained from the measured data fitting

Sample	Total radius (Å)	Maghemite (%)	-Fe_2O_3 (%)
A	40 ± 4	34 ± 5	66 ± 5
B	50 ± 5	26 ± 3	74 ± 3
C	58 ± 5	0 ± 8	100 ± 8

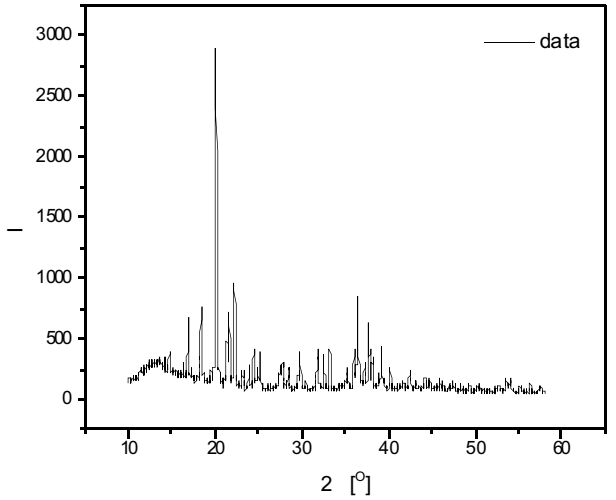

Figure 6. Sample D. Measured data of the sample annealed at the 1100 C as the highest temperature.

our fitting is not important. The fits describe the measured data well and the parameters of the core-shell model were obtained. The sample D (Fig. 6) could not have been fitted because of a too large size of the particles that made the simulation extremely time-consuming.

From the fitting of the measured data we obtained the total size of analyzed samples (A – C) and the fraction of the maghemite and phase assuming the core-shell model with maghemite as a core. It can be seen that the size of the particles increase with increasing annealing temperature and that the fraction of maghemite decreases and it completely vanishes at the temperature of 1000 C. This corresponds to the assumption presented above. As for the sample D, which has not been analysed, the hematite diffraction peaks appear.

Both he core-shell model of the nanoparticles and the Debye formula are suitable tools for the analysis of our samples. In the future we have to investigate, whether it is possible to distinguish between the core and the shell, i.e., whether we can determine which phase is in the core and which one is in the shell. A method, which would enable us to analyze larger particles, has to be implemented as well.

References

1. A. Cervellino, C. Giannini, A. Guagliardi and D. Zanchet, *Eur. Phys. J. B* **41** (2004), 485.
2. A. Cervellino, C. Giannini and A. Guagliardi, *J. Appl. Cryst.* **36** (2003), 1148.
3. Chang-Woo Lee, Sung-Soo Jung and Jai-Sung Lee, *Materials Letters* **62** (2008), 561.
4. M. Gich, C. Frontera, A. Roig et al, *Chemistry of Materials* **18** (2006), 3889.
5. P. Brázda, D. Nižňanský, J.-L. Rehspringer, J. Poltierová Vejpravová, *J. Sol-Gel Sci. Technol.*, **51** (2009), 78-83.

S5

RESIDUAL STRESS DETERMINATION BY LEAST SQUARE FITTING METHOD

Z. Pala[1], A. Sveshnikov[2], N. Ganev[1], K. Kolařík[1]

[1]Department of Solid State Engineering, Faculty of Nuclear Sciences and Physical Engineering, Czech Technical University in Prague, Trojanova 13, 120 00 Prague 2
[2]Department of Physics, Faculty of Civil Engineering, Czech Technical University in Prague, Thákurova 7, 166 29 Prague 6
zdenek.pala@fjfi.cvut.cz

Results of macroscopic residual stresses (RS) obtained from the X-ray diffraction tensometry are increasingly used for quality characterization of various surfaces and thin layers. In some cases even the depth distributions of RS are coveted as indispensable information about the processes of inhomogeneous plastic and thermal deformations which lead to the final shape of the studied object. Since the knowledge about the state of RS is highly desirable, the reliability and the accuracy of the macroscopic residual stress tensor components is an important topic in powder diffraction. The first concern, i.e. the *results' reliability*, is above all else given by the correspondence between the state of the measured object and the choice of experimental techniques and evaluation methods. The term "state of the measured object" encompasses not only the state of RS, i.e. biaxial or triaxial, but the object's real structure; particularly stress gradients, preferred orientation and grain size. Another vital feature of the stress results' reliability lies in the selection of the appropriate elastic constants as they directly link measured deformations with the stresses requested by the results' users. It is palpable that elastic constants are influenced by isotropy of the irradiated volume, mostly by the presence of texture and the history of plastic deformation. Calculation of elastic constants is a frequently tackled issue and the simple initial models of Voigt and Reuss [1] have been substantially modified over the last half century, the most advanced calculations consider interactions between crystallite and its inhomo-

geneous neighbourhood [2] and even presence of texture [3].

The benchmarks of the suitability of standard methods in RS determination, such as $\sin^2$, Dölle-Hauk and one tilt, are deviations from linearity of the so-called d versus $\sin^2$ plots. These plots depict dependence of interplanar lattice spacing of the chosen set of planes {hkl} in respect to the orientation of the diffraction vector to the surface normal given by the tilt and chosen azimuth :

$$\begin{aligned} {}^{L}_{33} \quad & \frac{d \quad d_0}{d_0} \quad \frac{1}{2} s_2 (\ {}^{S}_{11} \cos^2 \qquad {}^{S}_{12} \sin 2 \\ & {}^{S}_{22} \sin^2 \qquad {}^{S}_{33}) \sin^2 \\ & \frac{1}{2} s_2 (\ {}^{S}_{13} \cos \qquad {}^{S}_{23} \sin \ ) \sin 2 \\ & \frac{1}{2} s_2 \ {}^{S}_{33} \quad s_1 (\ {}^{S}_{11} \quad {}^{S}_{22} \quad {}^{S}_{33}) \end{aligned} \tag{1}$$

where d_0 stands for strain-free material, $0.5s_2$ and s_1 are X-ray elastic constants (XEC), the superscripts L and S stand for laboratory and sample coordinate system respectively. If d_0 is known the desired six components of macroscopic stress tensor $_{11}$, $_{22}$, $_{33}$, $_{13}$, $_{12}$, $_{23}$ can be calculated from the measured in six independent directions given by tilt and azimuth .

The *results' accuracy* can be substantially increased by measuring in more than six directions and by application of standard least-square fitting procedure. Detailed algorithm can be found in [4] and will be explained at length in the oral contribution. However, this is path is seldom followed and Dölle-Hauk method is used in vast majority of full stress tensor determination. Following Dölle-Hauk method, d versus $\sin^2$ plots are obtained for three azimuths. The selection of these azimuths itself is a topic for detailed analysis and recent papers, see e.g. [5], tend to prefer azimuths 0°, 60°, and 120° instead of commonly chosen 0°, 45°, and 90°. The fundamentals for this switch in measurement stereotype lies in the putatively smaller results' inaccuracies for the choice of the 0°, 60°, 120° combination.

It has been shown [6] that presence of pronounced texture and coarse grain in the measured polycrystalline material represent an impediment in RS determination by means of standard methods. Residual stress analysis in textured material is an especially arduous task, since its manifestations are oscillations in the d versus $\sin^2$ plots. Moreover, the texture is responsible for different elastic properties and hence the XEC are not the same as in non-textured materials. Residual stress determination by means of least-square fitting method is capable of taking texture into account if anisotropic XEC R_{ij}^{hkl} and X-ray stress factors F_{ij} are implemented into its algorithm [7, 8]. The equation (1) is then rewritten as

$${}^{L}_{33} \quad \frac{d \quad d_0}{d_0} \quad F_{ij} (\ , \ , R_{ij}^{hkl}) \ {}_{ij} \tag{2}$$

In order to assess and compare standard Dölle-Hauk method and residual stress determination by least-square fitting a ground sample of high carbon stainless steel M300 was investigated by XRD which was known to exhibit the so-called splitting and texture was virtually nonexistent [9]. For this purpose {211} diffractions of -Fe were investigated with CrK radiation (diffraction angle 2 156°) and X'Pert PRO MPD Bragg-Brentano diffractometer in -mode equipped with a proportional detector. The goniometer was adjusted in reference to a strain-free reference specimen of -Fe powder. The differential –method, when the azimuth is kept constant and the tilt is changing, was employed. Measurements were taken on the grinding direction = 0° and in further four azimuths defined by 45°, 60°, 90°, and 120°. For each azimuth seventeen tilts defined by $\sin^2$ = 0; 0.1; 0.2; ...0.8 were measured.

The aim was to obtain diffraction profiles of good and poor background to I_{max} ratio and subsequently to characterize the profiles measured in direction , by their centre of gravity. These data were subjected to residual stress calculation by Dölle-Hauk method and by least-square fitting using XEC calculated according to Eschelby-Kröner model. These procedures were imposed on two sets of data; the first consisted from azimuths 0°, 45°, and 90° and the other from 0°, 60°, and 120°. Even though the characterization of diffraction dublet by centre of gravity may seem obsolete in comparison with profile fitting methods, the [10] clearly shows that such treatment is suitable. Nevertheless, and only for comparison, the profiles were also fitted, after CrK $_2$ stripping, by Pearson VII function and its maximum then entered the residual stress calculations. The comparison of results' accuracy is performed on the basis of standard deviations.

References

1. I.C. Noyan, J.B. Cohen, *Residual Stress: Measurement by Diffraction and Interpretation.* New York: Springer. 1987.
2. H. Dölle, *J. Appl. Cryst.,* **12**, (1979), 489-501.
3. P.-O. Renault, E. Le Bourhis, P. Villain, Ph. Goudeau, K. F. Badawi, D. Faurie, *Appl. Phys. Lett.,* **83,** (2003), 473.
4. R.A. Winholtz, J.B. Cohen, *Aust. J. Phys.* , **41**, (1988), 189-199.
5. B. Ortner, *Int. J. Mat. Res.*, **98**, (2007), 87-90.
6. V. Hauk, *Structural and Residual Stress Analysis by Nondestructive Methods*. Elsevier. 1997.
7. B. Ortner, *J. Appl. Cryst.*, **39**, (2006), 401-409.
8. B. Ortner, *Z. Metallkd.*, **96**, (2005), 9.
9. Z. Pala, N. Ganev, *Mat. Sci. Eng. A*, **497**, (2008), 200-205.
10. H. Zantopulos, C. Jatczak, *Adv. X-ray Anal.*, **14**, (1971), 360 – 376.

Acknowledgements

The research was supported by the Project No 106/07/0805 of the Czech Science Foundation and by the Project MSM 6840770021 of the Ministry of Education, Youth and Sports of the Czech Republic.